

Vorticity Banding During the Lamellar-to-Onion Transition in a Lyotropic Surfactant Solution in Shear Flow

Georgina M. H. Wilkins and Peter D. Olmsted

School of Physics and Astronomy, University of Leeds, Leeds LS2 9JT, United Kingdom

Received: April 20, 2018/ Revised version: date

Abstract. We report on the rheology of a lamellar lyotropic surfactant solution (SDS/dodecane/pentanol/water), and identify a discontinuous transition between two shear thinning regimes which correspond to the low stress lamellar phase and the more viscous shear induced multi-lamellar vesicle, or “onion” phase. We study in detail the flow curve, stress as a function of shear rate, during the transition region, and present evidence that the region consists of a shear banded phase where the material has macroscopically separated into bands of lamellae and onions stacked in the vorticity direction. We infer very slow and irregular transformations from lamellae to onions as the stress is increased through the two phase region, and identify distinct events consistent with the nucleation of small fractions of onions that coexist with sheared lamellae.

PACS. 83. Rheology – 83.60.Wc Flow instabilities – 83.80.Qr Surfactant and micellar systems, associated polymers

1 Introduction

Surfactant lamellar phases have a wide range of flow - induced behaviour including shear thickening [1, 2], shear thinning [1, 3], shear induced structures [1, 2, 4] and shear-induced phase separation [1, 2, 4–9]. In one of the most dramatic transitions, discovered by Diat and Roux, shear flow can transform some lamellar phases can into multi-lamellar vesicles, or “onions” [1, 3]. In the SDS/ dodecane/ pentanol/ water system, stronger shear flow eventually destroys the onion phase in favour of either a highly aligned lamellar phase or multicylindrical “leek-like” structure [10]. This is an example of a shear induced microstructural phase transition. Other microstructural transitions have also been reported for lamellar phases made from different ingredients. For example, an SDS/ octanol/ brine mixture exhibits a transition from the lamellar to the sponge phase at 30°C [11]. At low imposed shear stresses the same system features a transition from a liquid onion phase to an ordered phase of onions organised into flat planes sliding over one another [12]. Conversely, for high enough shear rates, a certain SDS/ decanol/ water mixture undergoes a transition as a function of increasing decanol fraction, from the \hat{c} -orientation, consisting of lamellae that slide over each other with layer normals parallel to the flow gradient direction, to the \hat{a} -orientation, consisting of lamellae that lie in the shear plane with layer normals in the vorticity direction [13]. Interesting kinetics have been seen in other lyotropic lamellar phases, such as cylindrical or leek-like intermediates during the transition from lamellae to onions [9]. In this work we re-

visit the transition originally found by Diat and Roux in SDS/dodecane/pentanol/water, and study the lamellar-to-onion (L-O) transition region in more detail.

The onion phase is of great interest to the chemical industry: onions form in a variety of different surfactants and lipids, and the size is easily controlled by the magnitude of the applied shear rate $\dot{\gamma}$ or shear stress σ . As a result, onions can be designed for specific tasks such as micro-encapsulation of drugs or colour pigment. From an academic viewpoint, the shear-induced transition from lamellae to onions is a topology-changing transition that is still poorly understood, despite growing knowledge of defects in lamellar and condensed media [14]. Unresolved issues about the L-O transition include the mechanism of instability, physical nature of the transformation, possible phase coexistence between sheared lamellae and onions, the compatibility between onions and lamellar orientation, and the role of dislocations. We will argue below that the L-O transition is an example of “shear banding”, or separation of material into macroscopic bands of material. In this case the signatures are consistent with bands stacked along the vorticity direction, rather than the more conventionally seen layering in the flow gradient direction [15].

The best studied examples of shear banding are in solutions of entangled wormlike micelles in strong shear flows [16–19]. Flow induces an instability to a well-aligned and high viscosity state, such that under imposed strain rate conditions the fluid “phase separates” into macroscopic regions of material flowing at different shear rates, along a stress plateau that spans a range of shear rates (Fig. 1) [20]. The shear-induced band of lower viscosity

material increases in size as the average shear rate is swept across the plateau, and the shear bands are separated along the flow gradient direction (*gradient shear banding*), consistent with a common stress between bands. Gradient shear banding has been observed in dilute wormlike micelles using techniques such as magnetic resonance [21], ultrasonic velocity profiling [22] and optical birefringence microscopy [23].

Shear bands can also form along the vorticity direction (Fig. 1) [25]. This condition could be realized when two states, such as a fluid and induced gel, have multiple stresses for a range of strain rates. Phases with coexisting shear stresses do not violate the momentum balance as long as neighbouring bands are separated in the vorticity direction, although a normal stress condition must still be satisfied to determine the coexisting strain rate $\dot{\gamma}^*$. Thus, vorticity shear bands have different shear stresses whose sum must equal the total applied stress. For a shear thickening transition the corresponding rheological flow curve of such a material would exhibit a characteristic step increase of shear stress at a critical shear rate [24], as shown in Fig. 1.

The original work of Diat and Roux [3] showed a vertical step at a critical shear rate (in their most concentrated surfactant bilayer solution, $\phi_{oil} = 0.50$), which suggests that the SDS system is a candidate for vorticity banding. They also reported seeing structures along the vorticity direction, but in the range of shear rates associated with the transition between onions and the higher shear rate phase (either multicylindrical “leeks” or well aligned lamellae). Vorticity banding associated with a thinning transition, the alignment of a polydomain colloidal crystal in solution, was also been observed but not noted as such by Chen and Zukoski [26, 27]. More recently, Callaghan and co-workers, using magnetic resonance imaging, observed what is apparently a combination of vorticity and gradient banding in a semidilute wormlike micelle solution in a cone and plate geometry [28]. Fisher and co-workers have also observed structure formation along the vorticity direction in another wormlike micelle solution [29].

Here we study the shear induced microstructural L-O transition in the SDS system first studied by Diat and Roux, focusing on vorticity shear banding signatures. The paper is organised as follows. In section 2 we briefly describe the system and the experimental setup for measuring the rheology. In section 3, we summarise the homogeneous flow behaviour of the lamellar phase beginning with the low stress yield behaviour. In section 4 we study the macroscopic nature of the lamellar to onion transition and investigate effects of experimental protocol on the existence of the transition region. We finish with a discussion.

2 System and Experimental Details

2.1 Sample preparation

The lyotropic lamellar phase under study is a quaternary mixture of sodium dodecyl sulphate (SDS), pentanol, do-

decane and water. The materials were supplied by Aldrich Chemicals and used without further purification. Millipore multi-Q water with a resistivity better than 18.0 M Ω cm was used throughout. The lamellar phase is most easily obtained by diluting a concentrated lamellar phase (weight fractions of 47.4% water, 22.0% pentanol and 30.6% SDS) with an oil mixture (weight fractions of 92.0% dodecane and 8.00% pentanol). The lamellar phase exists along a very wide range of this dilution line. In Ref. [3] these two mixtures were first prepared separately and then mixed. Since this method often resulted in an inhomogeneous solution we mixed the required proportions of the constituent materials directly by shaking vigorously for several minutes. After shaking, the solution was placed in an oven at 60.0°C for several days.

At equilibrium, this phase comprises layers of water surrounded by surfactant separated by dodecane. Pentanol acts as a co-surfactant and occupies the oil part of the phase. At room temperature, the solution forms a lamellar phase for a large range of dodecane concentrations ($0.466 < \phi_{oil} < 0.644$, where ϕ_{oil} denotes the weight fraction of dodecane in the mixture) [30]. The bilayers are stabilised by thermal undulations [31], with a layer spacing d ranging from 5 nm to 20 nm depending on the concentration of the phase [3]. In this work we investigate lamellar phases with dodecane concentrations $\phi_{oil} = 0.466, 0.50, 0.569, 0.644$.

2.2 Rheology

A Rheometrics Scientific SR500 stress controlled rheometer was used throughout. A cone and plate geometry with a 40 mm diameter cone with angle $\alpha = 0.02$ radians was mounted on the rheometer stress head. A home-made Perspex solvent trap was used to minimize solvent evaporation. The plate was thermostatted using a water cooling system, and all experiments were performed at 24°C.

Sweep experiments are performed by imposing an initial stress after sample loading. The shear stress range is $0.1 \text{ Pa} < \sigma < 100 \text{ Pa}$. For larger stresses, depending on the concentration, the sample often spurted out of the cell, with the more viscous lamellar phases (lower ϕ_{oil}) being ejected at a lower stress. During the sweep experiments, successive stresses were imposed for either (a) a prescribed time τ_{max} or (b) until steady state criteria are reached. These criteria (or steady state test) identify an early steady state where the steady state is defined as the point where the shear rate $\dot{\gamma}$ remains within an “acceptance window”.

In the steady state test the measured shear rate is monitored as a function of the elapsed time since the previous stress increment. The steady state is defined according to the RMS fluctuations P of the shear rate around the mean shear rate,

$$P = \frac{\sqrt{\langle (\dot{\gamma} - \bar{\dot{\gamma}}(t))^2 \rangle_{5\%}}}{\bar{\dot{\gamma}}} \quad (1)$$

where the angle brackets and overbar denote a time average over the previous 5%(0.05 t) of the current duration t

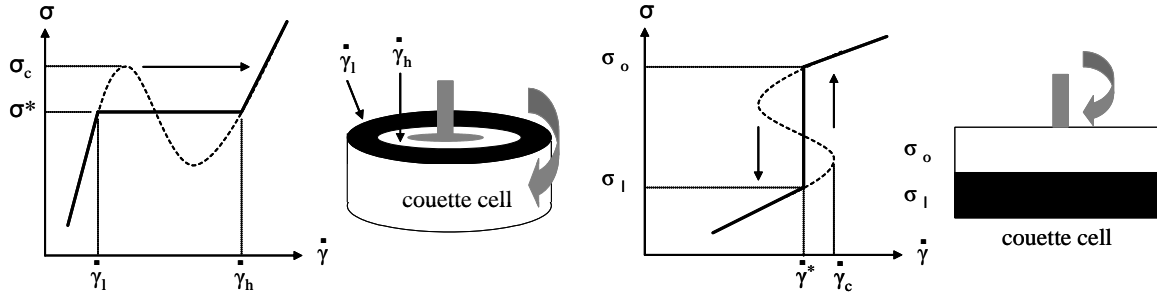


Fig. 1. Schematic flow curves for shear banding in cylindrical Couette geometry. Left: gradient banding, in which a high shear rate band flows near the inner cylinder and a low shear rate band flows near the outer cylinder. In ideal gradient banding the two phases coexist under imposed strain rate conditions, along the plateau at a selected shear stress σ^* . Right: Vorticity banding, in which the shear bands are stacked in the vorticity direction; in the ideal scenario shear bands coexist under controlled stress conditions, on a cliff at a selected strain rate $\dot{\gamma}^*$ [24]. In both cases the solid line shows the composite flow curve that would be measured in ideal shear banding, while the dashed line shows metastable (positive slope) or unstable (negative slope) portions of the constitutive curve. The arrows indicate some possible metastable pathways that could be followed for rapid experiments: such as rapidly increased stress in gradient banding, or rapidly decreased or increased strain rate in vorticity banding.

of the test. Typically the condition $P = 1\%$ or $P = 2\%$ was used. If the sample does not fall below set value for P within the maximum delay time τ_{max} , then the stress is incremented to the next stress in the series. Unless otherwise stated, $\tau_{max} = 2000$ s.

3 Non-linear rheology

Previous work on this system suggests the following succession of phases as a function of shear rate for the SDS/dodecane/pentanol mixture [1, 3, 7, 32–34]. An aligned smectic with no defects is solid like for flows that deform the layer spacing or induce bending, and fluid for flows that induce only layer sliding or in-layer flows. In principle a highly defected phase is solid-like with a yield stress due to defects; the yield stress is expected to be history dependent [35]. Upon applying a shear stress above the yield stress the layered phase flows, with layer alignment generally in the \hat{c} orientation, in which layer normals are parallel to the flow gradient direction [3]. The system flows until a critical shear rate or shear stress is reached (see below for a discussion), at which point the flowing lamellar phase is thought to undergo an undulation instability similar to the Helfrich-Hurault instability [1, 33, 36–38] to an onion phase. Candidate mechanisms for this undulation instability include local dilational stresses due to defects or wall asperities [1], “wrinkling out” of fluctuations into long wavelength modes in materials with no defects [38], or a change in preferred layer spacing due to reduced collisions, which leads to an effective dilational strain [36]. Following a discontinuous step in the shear rate, the sample is entirely converted to onions.

When the sample reaches a steady state the onions are monodisperse with radii R of the order of a few microns [1, 39]. The size can be heuristically understood as a balance of elastic deformation and viscous forces between onions

[1],

$$R = \sqrt{\frac{4\pi(2\kappa + \bar{\kappa})}{d\eta\dot{\gamma}}} \quad (2)$$

where κ and $\bar{\kappa}$ are the mean and Gaussian curvature moduli of the layers, η is a viscosity, and d is the smectic layer spacing. This approach works best when the viscosity used is the solvent viscosity rather than the apparent viscosity (*i.e.* flow only occurs between onions) [34]. Note that this argument does not address the mechanism by which onion sizes adjust, which involves other processes such as peeling and accretion of layers, internal layer collapse in the onions due to high internal stresses, and expulsion and absorption of solvent [40]. Panizza and co-workers measured the size to be

$$R = R_0 \left(\frac{\dot{\gamma}_0}{\dot{\gamma}} \right)^{-1/2}, \quad (3)$$

where $R_0 = 5.8 \mu\text{m}$ and $\dot{\gamma}_0 = 1 \text{ s}^{-1}$ when the dodecane oil concentration was $\phi_{oil} = 0.45$ [7]. The onions decrease in size with increasing shear rate, and at higher shear rates are unstable with respect to a well-aligned lamellar phase with few defects. The flow curves are consistent with a gradient banding coexistence of states along a stress plateau, although this coexistence has not been well-studied and the flow curves were measured using imposed stresses resulting in a discontinuity between the onion flow branch and the well aligned lamellar flow branch [3].

To illustrate these different regimes, figure 2 shows the flow curves measured using the sweep experiment protocol described above for oil concentrations $\phi_{oil} = 0.466$ (Fig. 2a and 2b) and $\phi_{oil} = 0.644$ (Fig. 2c). The apparent yield stress for the most concentrated membrane phase ($\phi_{oil} = 0.466$, which corresponds to a layer spacing $d \simeq 8.2 \text{ nm}$ [33]) is $\sigma_Y \simeq 0.13 \text{ Pa}$. Meyer *et al.* argued that the yield stress is that stress needed to deform a network of dislocations with average spacing ξ [39]:

$$\sigma_Y \sim \frac{1}{2} \frac{\bar{B}\bar{b}^3}{\xi^3}, \quad (4)$$

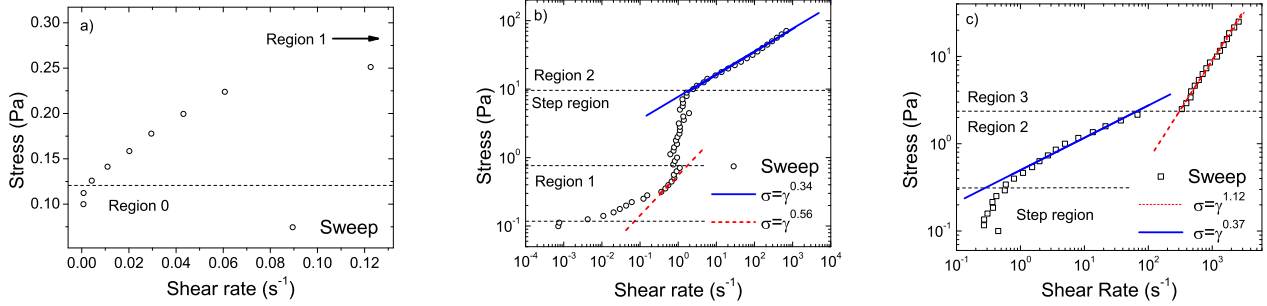


Fig. 2. Stress sweeps using the steady state criteria $\tau_{max} = 2000$ s and $P = 1\%$. Power laws are used to fit the different regions: a) and b) Stress sweep for $\phi_{oil} = 0.466$ (\circ). The material shows little deformation at imposed stresses below the yield stress ($\sigma_y = 0.12$ Pa). c) Stress sweep for the more dilute lamellar phase $\phi_{oil} = 0.644$ (\square).

where \bar{B} is the smectic compression modulus, and $\bar{b} \simeq b/(2\pi)$, where $b \simeq d$ is the Burger's vector of the dislocation. This leads to an estimated defect spacing of $\xi = 86$ nm with $\xi/d \simeq 11$ membranes between defects. Meyer and co-workers estimated $\xi/\bar{b} = 65$ for a thermotropic system (8CB), and $\xi/\bar{b} = 8$ for a lyotropic system (quasi-ternary ammonium surfactant cetylpyridinium chloride, hexanol and brine), quite close to the value we find in the SDS solution.

After yielding, the $\phi_{oil} = 0.466$ sample flows with severe shear thinning from σ_Y to $\sigma \simeq 0.3$ Pa (Region 1, Fig. 2 b). Depending on the region of fitting, the flow curve may fit a power law,

$$\sigma \sim \dot{\gamma}^{n_l}, \quad (5)$$

where $n_l \simeq 0.56$ when the data are fit over the range $1 \times 10^{-1} < \dot{\gamma} < 1 \times 10^0$, but $n_l \simeq 0.26$ if the data are fit over the range $1 \times 10^{-2} < \dot{\gamma} < 1 \times 10^{-1}$. Hence the data do not reliably support one particular power law. The shear thinning behaviour in region 1 exhibits a small yet reproducible discontinuous jump in the shear rate, similar to a stress plateau, that separates the different power law fits. This could be related to wall slip or some complicated yielded banded flow as recently proposed by Picard and co-workers [41]. This type of complex behaviour could explain the difficulty in reaching a steady state. An exponent of $n_l = 0.6$ was predicted by Meyer *et al.* [39] and Colby [35] for defected lamellar phases by adapting the Orowan equation for high temperature creep due to defects in metals and alloys to describe plastic flow of defected lamellae. Similar arguments were recently used in [42] in a phase of defected hexagonal micelles.

We will argue below that the stress step, or cliff, near $\dot{\gamma}_c$ corresponds to a coexistence of lamellae and onions. The putative onion-lamellae coexistence region spans stresses $\sigma_l \simeq 0.3$ Pa to $\sigma_o \simeq 1$ Pa at a strain rate $\dot{\gamma}_c \simeq 1$ s $^{-1}$ for $\phi_{oil} = 0.466$, followed by the homogeneous onion phase (region 2) at higher stresses. The onion phase shear thins according to

$$\sigma \sim \dot{\gamma}^{n_o}, \quad (6)$$

where $n_o \simeq 0.34$. This result agrees with studies on similar systems [1, 2, 39, 43]. In the dilute sample the onion microstructure is apparently destroyed at high stresses, and is replaced by a structure (region 3) whose behaviour is closer to Newtonian, $\sigma \sim \dot{\gamma}$ [3]. The flow curve in the transition between regions 2 and 3 is consistent with gradient shear banding, but we have not studied this in detail. A stress plateau would only be seen under controlled shear rate conditions. Another possibility is vorticity banding in which the high shear rate phase has a lower stress; in this case a negative apparent flow curve could be seen under controlled strain rate conditions [24]. The high shear lamellar phase is only measurable by the SR500 rheometer for the most dilute lamellar phase ($\phi_{oil} = 0.644$). For more concentrated systems the transition occurs at a higher stress [3] and the sample was expelled from the cone and plate geometry before this region was reached. We do not know whether this is an inertial, surface, or normal stress instability.

The stress σ_l at which the lamellae to onion transition occurs decreases weakly with increasing oil fraction, or equivalently decreasing layer spacing (Fig. 3). Hence, more dilute lamellar phases appear to require a lower stress to induce the onion phase.

The measured rheology between region 1 (lamellae) and region 2 (onions) depends upon the experimental protocol. Figure 4 shows stress sweeps at increasing sweep times from $\tau_{s/d} = 100$ s to $\tau_{s/d} = 2500$ s where $\tau_{s/d}$ is the sweep time calculated from the number of seconds per decade of imposed stresses. The shear rate at which the stress cliff occurs decreases as $\tau_{s/d}$ is increased. The non-monotonic 'S' bend present in all the non-equilibrium flow curves. The S bend appears to shift to lower stresses for slower sweeps, which implies that the lamellar phase can lose stability quite slowly, and is broadly similar to nucleated behaviour. Stress sweeps with sweep times $\tau_{d/s} > 200$ s exhibit two features in the shear rate cliff. The first, already noted, is the nonmonotonic S bend and occurs at the termination of region 1. The second is the vertical 'shoulder' which occurs before the beginning of region 2. The shoulder is most prominent for the slowest sweeps.

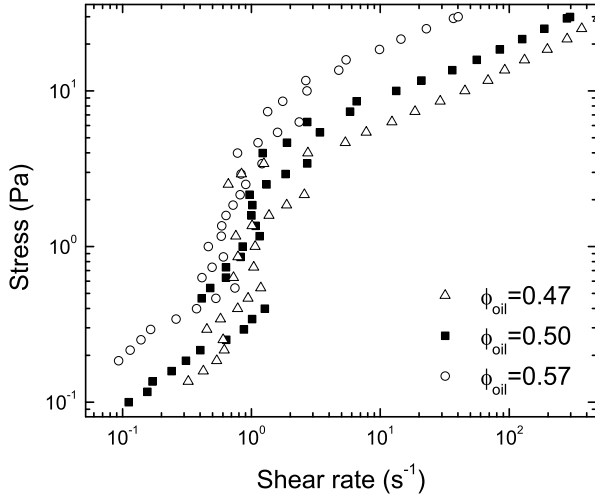


Fig. 3. Stress sweep flow curves for a range of oil concentrations. All the sweeps were performed using sweep criteria $\tau_{max} = 2000$ s and $P = 1\%$.

The slowest sweeps ($\tau_{s/d} = 2000$ s and $\tau_{s/d} = 2500$ s) almost superpose during the step region, with the S bend and the shoulders occur at similar shear rates.

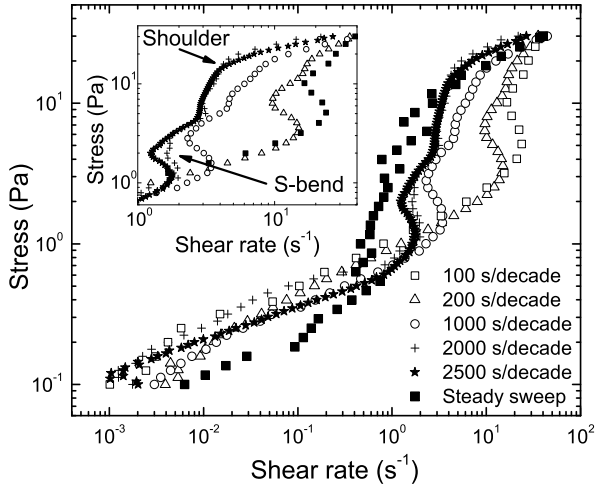


Fig. 4. Stress sweeps for $\phi_{oil} = 0.47$. The time per stress increment is varied from $\tau_{max} = 10 - 100$ s and the number of stress increments per decade is varied from 10 to 50 points per decade, and the total time per decade is quoted on the plot. Inset: enlargement near the S bend. As a comparison, data is also shown for a stress sweep with steady state conditions $\tau_{max} = 2000$ s and $P = 1\%$ (■).

The slope of the low stress lamellar phase branch changes with the sweep time. The branches are fit with the power

Table 1. Power law exponents for the lamellar flow branch from figure 4, together with the sweep time per decade ($\tau_{s/d}$) and the stress σ_{sh} and shear rate $\dot{\gamma}_{sh}$ at the top of the shoulder in the step region.

$\tau_{s/d}$	σ_{sh} (Pa)	$\dot{\gamma}_{sh}$ (s^{-1})	n_l
100	30.0	40.3	0.342
200	23.9	16.9	0.338
1000	19.1	10.7	0.283
2000	16.3	4.2	0.246
2500	16.3	4.2	0.235

law $\sigma \sim \dot{\gamma}^{n_l}$ where the exponent n_l ranges from $0.235 < n_l < 0.342$ depending on the sweep time (Table 1). The slowest stress sweeps shear thin with the smallest exponent, $n_l \sim 0.235$, which could indicate that fewer defects have been produced or that more defects have been removed. The transformation from lamellae to onions is thus very slow. A couple of possible mechanisms could be: (1) a Helfrich-Hurault like undulatory instability that grows slowly and takes a long time to convert to onions; or (2) a slow nucleation process. The flow curves measured for the slow stress sweeps reach the onion flow branch at lower shoulder stresses (σ_{sh}) as shown in the table and figure. Perhaps this is due to the slow conversion to onions, such that for fast sweeps the conversion occurs at larger σ_{sh} .

We can also interpret the S bend described above as a feature associated with the formation of onions. The backwards S is consistent with progressive stress inducing more onions hence decreasing the shear rate. The forwards S at higher stresses implies that any contribution to the measured shear rate from conversion of lamellae to onions (which would lead to decreasing shear rate) is overwhelmed by the tendency of the onions to act normally and flow faster. Since there are many more onions at higher stresses their effect is far greater.

4 Evidence for vorticity shear banding

4.1 Flow segments and discontinuous shear rate jumps

We have shown above that the measured flow curve is very sensitive to the sweep time in the region of the lamellar to onion transition, in the step region. In this section we focus in more detail on the rheology in this region. Stress sweeps were performed with 15 stress increments per decade and a maximum stress step time of $\tau_{max} = 2000$ s giving a maximum sweep time of $\tau_{d/s} = 30000$ s, which is significantly longer than the sweep times applied above (Fig. 4). The steady state condition was set to $P = 1\%$.

Figure 5 presents flow curves with sweep criteria $\tau_{max} = 2000$ s and $\tau_{max} = 4000$ s. It is clear that slower sweeps (larger τ_{max}) produces a more vertical step region. However, increasing τ_{max} does not significantly alter the flow curves in region 1 and region 2; this contrasts what we reported for fixed time stress sweeps (see Fig. 4) where altering the sweep time ($\tau_{d/s}$) affected both the slope of

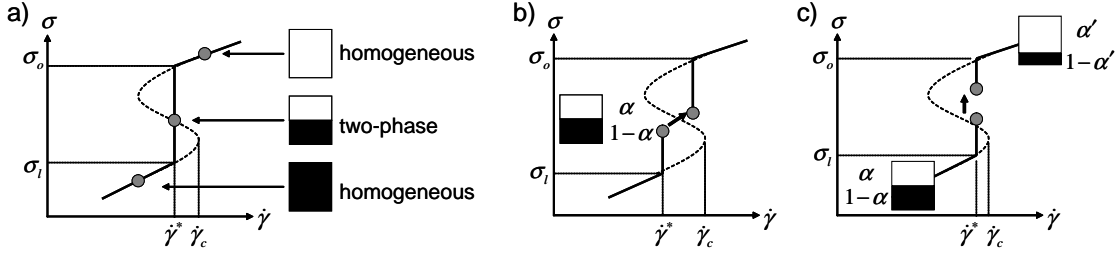


Fig. 8. a): Flow curve showing three possible states; two homogeneous and one vorticity banded, in an ideal situation in which the two states coexist at a “selected” shear rate $\dot{\gamma}^*$. Two possible scenarios are shown for the evolution of a vorticity-banded configuration upon increasing the stress. In b) the fraction of material α in the onion branch stays the same, and the two phases evolve along their respective flow branches, hence increasing the shear rate $\dot{\gamma}$ above $\dot{\gamma}^*$. In c) α increases to α' after which the system returns to the selected strain rate $\dot{\gamma}^*$.

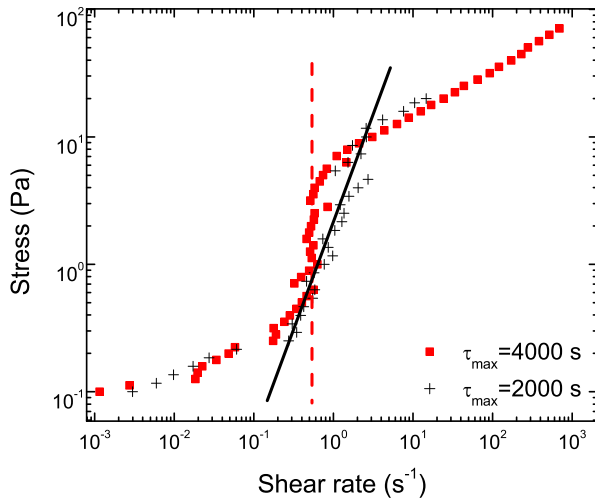


Fig. 5. Stress sweeps for $\phi_{oil} = 0.50$. Steady state conditions were different for the two sweeps; when $\tau_{max} = 2000$ s, $P = 1\%$ and when $\tau_{max} = 4000$ s, $P = 0.1\%$.

the flow curve in region 1 and the step region. Furthermore, the critical shear rate $\dot{\gamma}^*$ is similar for both sweeps regardless of the duration of τ_{max} ($\dot{\gamma}^* = 0.31 \text{ s}^{-1}$ for the faster sweep and $\dot{\gamma}^* = 0.51 \text{ s}^{-1}$ for the slower).

Figure 5 indicates jagged behaviour during the step region, during which the measured shear rate oscillates between $\dot{\gamma}^*$ and a larger shear rate. The fast stress sweep is more jagged than the slow sweep. On closer inspection of the step region one notices a series of intermediate flow segments with slopes slightly steeper than the lamellar constitutive curve, separated by discontinuous jumps to lower shear rates as the stress is increased.

Figures 6 and 7 show the measured flow curves for a stress sweep of a sample with $\phi_{oil} = 0.466$. The jagged behaviour described earlier is apparent in the step region. Also plotted is the steady state time τ_{ss} , which is the time necessary to reach the steady state condition $P = 1\%$. Along the lamellar and onion flow branches τ_{ss} is always

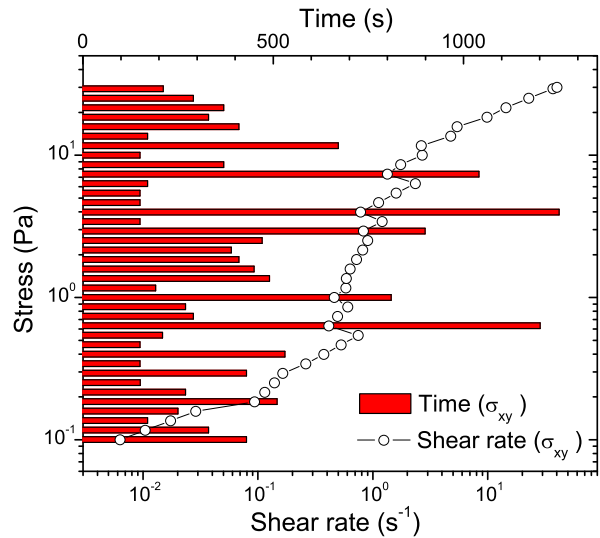


Fig. 6. Stress sweep for $\phi_{oil} = 0.466$ using the steady state criteria $\tau_{max} = 2000$ s and $P = 1\%$. The horizontal bars denote the time the material required to reach a steady state within the criterion $P = 1\%$.

a few hundred seconds, and remains fairly constant for subsequent stress increments. However, during the step region τ_{ss} varies widely, $150 \text{ s} < \tau_{ss} < 1200 \text{ s}$. There is a strong correlation between τ_{ss} and the jagged shape of the step region. Long steady state times occur for jumps, *i.e.* stress steps that lead to a decrease in shear rate; while the shorter steady state times correspond to moving along the flow segments and increasing the strain rate. This correlation between τ_{ss} and jumps and flow segments occurs for stress sweeps of all the concentrations studied and is reproducible.

The step region itself is broadly consistent with vorticity banding between the quiescent lamellar phase and thicker flow-induced onion phase, and we will argue below that the jagged behaviour is due to very slow and com-

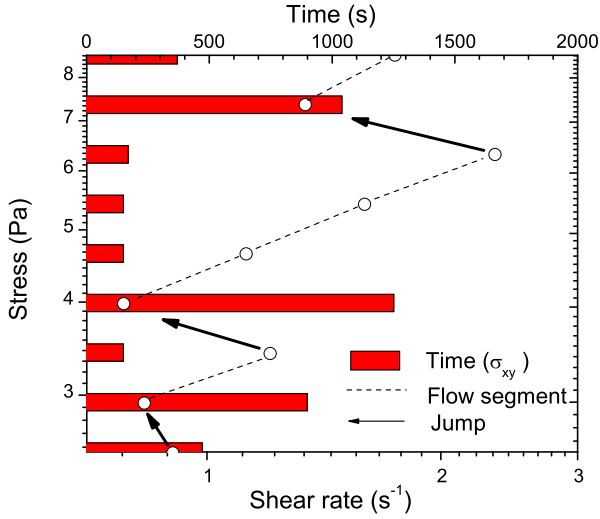


Fig. 7. Enlargement of the top of the step region in figure 6. The flow segments are shown as dotted lines and the jumps are shown with arrows.

plex transformation kinetics between lamellar and onion states.

4.2 Model for stress evolution during vorticity banding

In a vorticity banded state the total imposed stress $\bar{\sigma}$ must equal the sum of the individual stresses in the shear bands,

$$\bar{\sigma}(\dot{\gamma}) = \alpha\sigma_O(\dot{\gamma}) + (1 - \alpha)\sigma_L(\dot{\gamma}), \quad (7)$$

where α is the fraction of material in the onion state (converted from lamellae) and $\sigma_O(\dot{\gamma})$ and $\sigma_L(\dot{\gamma})$ are the constitutive relations of the onion and lamellae shear band respectively. In true steady state the shear rate $\dot{\gamma}^*$ at which coexistence between lamellae and onions can occur may be uniquely selected [15,44], by analogy with the shear stress that is apparently selected in gradient banding [45,46]. For materials whose coexisting states have the same concentration the selected shear rate is predicted to be independent of concentration, resulting in a stress “cliff”; while materials in which the coexisting state have different concentrations may have a selected shear rate $\dot{\gamma}^*$ that depends on stress, or equivalently on α [15,24].

For the sake of argument, we first suppose that lamellar-onion coexistence has an ideal constant selected shear rate $\dot{\gamma}^*$ independent of stress. Consider a vorticity-banded state at a given stress σ and shear rate $\dot{\gamma}^*$, with some fraction α of onion material. Upon increasing the stress there are two possibilities:

(i) α can remain fixed, with the onion and lamellar phases increasing their shear rates to accommodate the increased stress, and hence following their respective constitutive curves. Successive stresses would lead to a

flow branch intermediate between the lamellar and onion branches, given by Eq. (7), as shown in Fig. 8b.

(ii) α can increase as lamellae convert to onions and the shear rate eventually returns to the selected value $\dot{\gamma}^*$. This could occur if the lamellar phase no longer “absorbs” the increased strain rate demanded by the stress, but responds either by an instability of by nucleating new onion material (Fig. 8c).

Scenario (i) is consistent with the evolution along flow segments that we find, while scenario (ii) is consistent with the jumps between flow segments. To test this we have extracted the rheology of the lamellar ($\sigma_L(\dot{\gamma})$) and onion ($\sigma_O(\dot{\gamma})$) branches, and shown the expected rheology of a heterogeneous mixture that evolves at constant onion fraction α , according to Eq. (7), in Fig. 9 for different onion fractions α . It is clear that some of the flow segments follow the fixed α flow branches quite well. Fig. 10 shows sweeps with different steady state times τ_{ss} ; it is apparent that the two experiments yield similar behavior, but the onset transition is at a lower strain rate for the slower experiment.

This simple picture would, of course, be complicated by very slow transformation kinetics between states. Moreover, it appears that the coexistence strain rate, if there is one, is not constant but slowly increases with stress. This might be expected for a solution, in which the coexistence conditions can be expected to depend on concentration, which leads to a stress-dependent selected strain rate because of a biphasic window in the equivalent non-equilibrium strain rate-concentration phase diagram [24,25]. We stress the fact that no such phase diagram has been calculated for a lyotropic lamellar system, and that these data are merely consistent with such a phase diagram.

This behaviour of the L-O transition should be contrasted with the well-known kinetic behaviour seen in gradient banding fluids such as wormlike micelles [47–50]. Wormlike micelles can phase separate into two bands along a stress plateau for a range of shear rates (Fig. 1a). Upon increasing the shear rate while on the plateau the systems invariably return to the stress plateau, corresponding to an increase in the fraction α of the high shear rate phase [50]. By contrast, the SDS mixture we study appears to get “stuck” in the low stress lamellar phase much more easily than the micellar phase gets stuck in the low shear rate phase. There are several possible contributing factors for this:

1. In a vorticity-banded state the interface lies in the shear plane, while in a gradient banded state the shear flow occurs across, rather than within, the interface. The lack of a direct shear force across the interface could lead to slower interface motion.
2. The lamellar and onion phases are not smoothly related by a continuous order parameter; hence one may expect that nucleation-like behavior, should it occur under flow, would be very slow. One candidate for onion formation is a critical shear rate for an undulation instability; it is possible that this instability can be preempted by finite amplitude fluctuations which

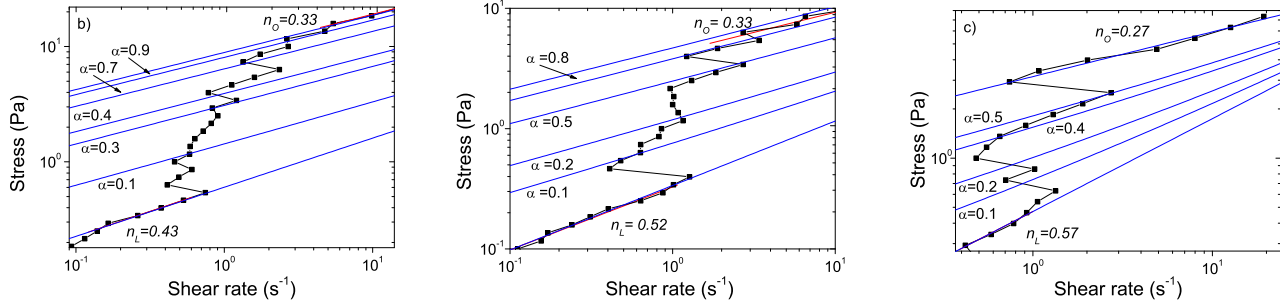


Fig. 9. Stress sweeps using steady state criteria $\tau_{max} = 2000$ s and $P = 1\%$. Power laws are plotted with different α values according to Eq. 7: a) $\phi_{oil} = 0.466$, b) $\phi_{oil} = 0.50$, c) $\phi_{oil} = 0.569$.

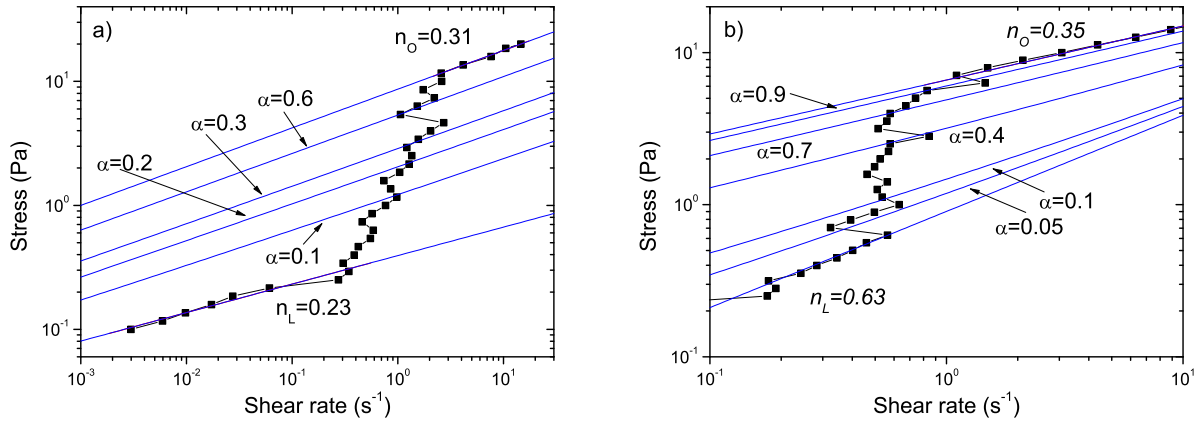


Fig. 10. Stress sweeps using different steady state criteria; a) $\tau_{max} = 2000$ s and $P = 1.0\%$, b) $\tau_{max} = 4000$ s and $P = 1.0\%$. Both sweeps were carried out on lamellar phases with oil concentration $\phi_{oil} = 0.50$.

can nucleate onions below the critical shear rate for the instability, but that these fluctuations are very slow. In the wormlike micellar systems such a nucleation barrier, if there is one, is apparently relatively easy to overcome [47–50].

3. Vorticity banding would present an interface that has no preferred position with reference to the flow geometry. By contrast, gradient banding in cylindrical Couette or cone and plate geometries leads to an interface that lies in a stress gradient set by the curvature of the flow. This stress gradient effectively drives the interface to move until it is at the position of the selected stress σ^* [50, 51]. There is no such driving force for vorticity banding, which again leads to slow kinetics.

In the steady state tests the times between data points provide further evidence for this interpretation (Fig. 6 shows the time to reach steady state τ_{ss} as bars). During flow segments each stress step requires only a few hundred seconds at most before the steady state criteria are satisfied. The discontinuous shear rate “jump” to a lower shear rate takes a long time to reach a steady state within the set criteria. Flow segments are thought to be associated

with no or very small changes in microstructure, and shear rate jumps related to events where lamellae are converted to onions. Hence, the time to reach a quasi-steady state at fixed α should be governed by the processes associated with moving along the homogeneous flow branches of the lamellar and onion phases. In the lamellar phase this involves changing the steady state defect density [39], while in the onion phase the onion size should decrease [3]. The very large steady state time indicates a rapid initial change in conditions upon the first thickening event, followed by a slow relaxation to steady state. This would include, in the case of onion formation associated with an increased α , the formation of an entire new band of onion phases around the entire circumference of the rheometer, as well as a return of all onion sizes to the larger size expected at the lower shear rate.

To summarise: we suggest that the flow segments correspond to an increasing stress in which the fraction of onion material remains fixed, separated by discrete jump decreases in shear rate that correspond to the formation of new bands of onions. We attribute the slow and irregu-

lar /non-reproducible behaviour to the nucleation-like behaviour of onion formation for small increases in stress.

5 Conclusions

In this work we have studied the rheology of a lyotropic lamellar system undergoing a transition between lamellar and multi-lamellar, or “onion”, phases. The transition is discontinuous, and the flow curves $\sigma \simeq \dot{\gamma}^n$ follow distinct forms in the different phases: in the lamellar regime $\sigma \sim \dot{\gamma}^{0.6}$ (depending on the region of fitting), and in the onion regime $\sigma \sim \dot{\gamma}^{0.3}$. The latter is consistent with previous measurements [52], while the former is consistent with theory and experiment [53]. We have also identified a very low strain rate signature consistent with yield due to a defect network, from which we estimate defect spacings consistent with previous work on lyotropic lamellar phases [39].

The discontinuity in the measured shear stress at a given shear rate is a “cliff”, analogous to the stress plateau found in the better understood wormlike micelle system. In shear thinning wormlike micelles the stress plateau indicates macroscopic phase separation into bands of material flowing with different local shear rates; while the cliff in the lamellar/onion case is consistent with bands lamellae and onions stacked in bands along the vorticity axis, which have the same shear rate but different shear stresses. Using a simple model for the superposition of the stresses in the two phases at coexistence, we are able to understand the noisy behaviour along the plateau as due to nucleation (or instability and subsequent slow growth) of onions out of the lamellar phase. Because nothing is expected to break the symmetry along the vorticity axis, we do not expect two large macroscopic bands (of the two phases), but rather a much finer dispersion of bands. Although other groups have reported vorticity banding in colloidal suspensions [26,27] and wormlike micelles [28,29], this is the first explicit attempt to understand the rheology of such a phase separated state.

In another previous study of a lyotropic lamellar system, Bonn *et al.* visualized vorticity banding in AOT, during transient experiments [54]. The flow curves in that case exhibited apparent shear thinning, and it is not apparent how the reported bands related to the overall steady state of the materials. Nonetheless, there are probably similar phenomena occurring, at least in part, in the two systems.

Our results thus strongly suggest that the lamellar to onion transition for the quaternary mixture of SDS, water, pentanol and dodecane exhibits vorticity shear banding. Direct observation of the lamellar phase in the vorticity-flow plane during stress controlled shear is necessary to confirm this hypothesis along with further study on the microstructure of the shear bands and this work is currently in progress. Initial birefringence studies indicate vorticity shear bands of differing anisotropies exist in the shear region.

We thank the UK EPSRC for financial support, and R. Colby, S. Manneville, J. Dhont and P. Lettinga for advice.

We are especially grateful to S. Lerouge for invaluable guidance during the early stages of this work.

References

1. D. Roux, F. Nallet, and O. Diat, *Europhys. Lett.* **24**, 53 (1993).
2. J. Bergenholtz and N. J. Wagner, *Langmuir* **12**, 3122 (1996).
3. O. Diat, D. Roux, and F. Nallet, *J. Phys. II (France)* **3**, 1427 (1993).
4. O. Diat, D. Roux, and F. Nallet, *J. Phys. I (France)* **3**, 193 (1993).
5. H. Hoffmann, *ACS Symposium Series* **578**, 2 (1994).
6. J. M. Franco, J. Munoz, and C. Gallegos, *Langmuir* **11**, 669 (1995).
7. P. Panizza, A. Colin, C. Coulon, and D. Roux, *European Physical Journal B* **4**, 65 (1998).
8. H. Mahjoub, K. McGrath, and M. Kleman, *Langmuir* **12**, 3131 (1996).
9. F. Nettesheim, J. Zipfel, U. Olsson, F. Renth, P. Lindner, and W. Richtering, *Langmuir* **19**, 3603 (2003).
10. A. S. Wunenburger, A. Colin, T. Colin, and D. Roux, *Eur. Phys. J. E* **2**, 277 (2000).
11. P. Herve, D. Roux, A. M. Bellocq, F. Nallet, and T. Gullikrzywicki, *J. Phys. II* **3**, 1255 (1993).
12. P. Sierro, Ph.D. thesis, University of Bordeaux, 1995.
13. J. Zipfel, P. Berghausen, P. Linder, and W. Richtering, *J. Phys. Chem. B* **103**, 2841 (1999).
14. M. Kleman and O. D. Lavrentovich, *Soft Matter Physics: an introduction* (Springer-Verlag, New York, 2003).
15. P. D. Olmsted and C.-Y. D. Lu, *Phys. Rev.* **E60**, 4397 (1999).
16. A. Khatory, F. Lequeux, F. Kern, and S. J. Candau, *Langmuir* **9**, 1456 (1993).
17. H. Rehage and H. Hoffmann, *Mol. Phys.* **74**, 933 (1991).
18. M. E. Cates, *J. Phys. Chem.* **94**, 371 (1990).
19. M. E. Cates, *J. Phys. Cond. Matt.* **8**, 9167 (1996).
20. N. A. Spenley, M. E. Cates, and T. C. B. McLeish, *Phys. Rev. Lett.* **71**, 939 (1993).
21. P. T. Callaghan, M. E. Cates, C. J. Rofe, and J. B. A. F. Smeulders, *J. Phys. II (France)* **6**, 375 (1996).
22. L. Becu, S. Manneville, and A. Colin, *Phys. Rev. Lett* **93**, 018301 (2004).
23. S. Lerouge, J. Decruppe, and C. Humbert, *Physical Review Letters* **81**, 5457 (1998).
24. P. D. Olmsted, *Europhys. Lett.* **48**, 339 (1999).
25. P. D. Olmsted and C. Y. D. Lu, *Phys. Rev.* **E 56**, R55 (1997).
26. L. B. Chen, C. F. Zukoski, B. J. Ackerson, H. J. M. Hanley, G. C. Straty, J. Barker, and C. J. Glinka, *Phys. Rev. Lett.* **69**, 688 (1992).
27. L. B. Chen, M. K. Chow, B. J. Ackerson, and C. F. Zukoski, *Langmuir* **10**, 2817 (1994).
28. M. Britton and P. Callaghan, *Eur. Phys. J. B* **7**, 237 (1999).
29. E. K. Wheeler, P. Fischer, and G. G. Fuller, *J. Non-Newton. Fl. Mech.* **75**, 193 (1998).
30. C. Safinya, D. Roux, G. Smith, S. Sinha, P. Dimon, N. Clark, and A. Bellocq, *Phys. Rev. Lett.* **57**, 2718 (1986).
31. D. Roux and C. R. Safinya, *J. Phys (France)* **49**, 307 (1988).

32. C. Cristobal, J. Rouch, P. Panizza, and T. Narayanan, *Phys. Rev. E* **6401**, 011505 (2001).
33. L. Courbin, J. P. Delville, J. Rouch, and P. Panizza, *Phys. Rev. Lett.* **89**, 148305 (2002).
34. L. Courbin and P. Panizza, *Physical Review E* **69**, 021504 (2004).
35. R. H. Colby, L. M. Nentwich, S. R. Clingman, and C. K. Ober, *Europhysics Letters* **54**, 269 (2001).
36. S. W. Marlow and P. D. Olmsted, *Eur. Phys. J. E.* **8**, 485 (2002).
37. A. S. Wunenburger, A. Colin, J. Leng, A. Arneodo, and D. Roux, *Phys. Rev. Lett.* **86**, 1374 (2001).
38. A. G. Zilman and R. Granek, *Eur. Phys. J. B* **11**, 593 (1999).
39. C. Meyer, S. Asnacios, M. Kleman, and C. Bourgaux, *Rheologica Acta* **39**, 223 (2000).
40. A. Leon, D. Bonn, and J. Meunier, *Journal of Physics: Condensed Matter* **14**, 4785 (2002).
41. G. Picard, A. Ajdari, F. Lequeux, and L. Bocquet, *Physical Review E* **71**, 010501 (2005).
42. L. Ramos and F. Molino, *Physical Review Letters* **92**, 018301 (2004).
43. L. Courbin, P. Panizza, and J. B. Salmon, *Physical Review Letters* **92**, 018305 (2004).
44. J. L. Goveas and P. D. Olmsted, *Eur. Phys. J.* **E6**, 79 (2001).
45. P. D. Olmsted and P. M. Goldbart, *Phys. Rev.* **A46**, 4966 (1992).
46. C. Y. D. Lu, P. D. Olmsted, and R. C. Ball, *Phys. Rev. Lett.* **84**, 642 (2000).
47. J. F. Berret and G. Porte, *Phys. Rev.* **E 60**, 4268 (1999).
48. J. F. Berret, *Langmuir* **13**, 2227 (1997).
49. C. Grand, J. Arrault, and M. E. Cates, *J. Phys. II (France)* **7**, 1071 (1997).
50. O. Radulescu, P. Olmsted, J. Decruppe, S. Lerouge, J.-F. Berret, and G. Porte, *Europhysics Letters* **62**, 230 (2003).
51. P. D. Olmsted, O. Radulescu, and C.-Y. D. Lu, *J. Rheology* **44**, 257 (2000).
52. D. Roux, F. Nallet, and O. Diat, *Europhys. Lett.* **24**, 53 (1993).
53. C. Meyer, S. Asnacios, and M. Kleman, *Eur. Phys. J. E* **6**, 245 (2001).
54. D. Bonn, J. Meunier, O. Greffier, A. Alkhwaji, and H. Kellay, *Phys. Rev.* **E 58**, 2115 (1998).